

UNCLASSIFIED

Defense Technical Information Center  
Compilation Part Notice

ADP012851

TITLE: Single Photon Turnstile Device

DISTRIBUTION: Approved for public release, distribution unlimited  
Availability: Hard copy only.

This paper is part of the following report:

TITLE: Nanostructures: Physics and Technology International Symposium  
[6th] held in St. Petersburg, Russia on June 22-26, 1998 Proceedings

To order the complete compilation report, use: ADA406591

The component part is provided here to allow users access to individually authored sections of proceedings, annals, symposia, etc. However, the component should be considered within the context of the overall compilation report and not as a stand-alone technical report.

The following component part numbers comprise the compilation report:  
ADP012712 thru ADP012852

UNCLASSIFIED

## Single photon turnstile device

Y. Yamamoto<sup>†‡</sup>, J. Kim<sup>†</sup>, O. Benson<sup>†</sup> and H. Kan<sup>§</sup>

<sup>†</sup> ERATO Quantum Fluctuation Project, Edward L. Ginzton Laboratory, Stanford University, Stanford, CA 94305, USA

<sup>‡</sup> NTT Basic Research Laboratories, 3-1 Morinosato-Wakamiya Atsugi, Kanagawa, 243-01, Japan

<sup>§</sup> ERATO Quantum Fluctuation Project, Hamamatsu Photonics Inc., Hamamatsu, Shizuoka, Japan

**Abstract.** A single-photon turnstile device based on a simultaneous Coulomb blockade effect for electrons and holes was demonstrated in a mesoscopic double-barrier  $p$ – $n$  junction. The current-voltage characteristics at 50 mK featured three plateaus at  $I = ef$ ,  $2ef$ , and  $3ef$ , where  $f$  is an external modulation frequency. The emitted photon was detected by a Si solid-state photomultiplier with a quantum efficiency of  $\geq 90\%$ , multiplication gain of  $\sim 30,000$ , response time of  $\sim 2$  ns, and absolutely no excess noise. The emitted photons at the first current plateau were well localized at the rising edge of the driving pulse as expected.

### 1 Introduction

Quantum interference between indistinguishable quantum particles profoundly affects their arrival time and counting statistics. Photons from a thermal source tend to arrive together (bunching) and their counting distribution is broader than the classical limit (super-Poissonian or super-shot noise) [1]. Electrons from a thermal source, on the other hand, tend to arrive separately (anti-bunching) and their counting distribution is narrower than the classical limit (sub-Poissonian or sub-shot noise) [2, 3, 4]. Manipulation of quantum statistical properties of photons with various non-classical sources is at the heart of quantum optics: Fermionic features such as anti-bunching, sub-Poissonian and squeezing (sub-shot noise) behaviors were demonstrated for photons. While only one electron can occupy a single state due to the Pauli exclusion principle and thus the electrical conductance for a ballistic single-mode channel is quantized to  $G_0 = 2e^2/h$ , no similar effect for photons exists [5, 6, 7]. Here we report the first realization of such a quantized photon flux, i.e., a single-photon stream with a well-regulated time interval.

Recent mesoscopic physics experiments demonstrated that an ultra-small tunnel junction regulates the electron transport one-by-one due to the large single-charging energy compared to the thermal background energy [8, 9, 10]. This stimulated an interesting question of whether such single-electron control techniques can be extended to single-photon manipulation.

### 2 Principle of single-photon turnstile device

A single-photon turnstile device utilizes a simultaneous Coulomb blockade effect for electrons and holes in a mesoscopic double barrier  $p$ - $n$  junction [Fig. 1(a)]. The structure consists of an intrinsic central quantum well (QW) in the middle of a  $p$ - $n$  junction and the  $n$ -type and  $p$ -type side QWs isolated by tunnel barriers from the central QW. The

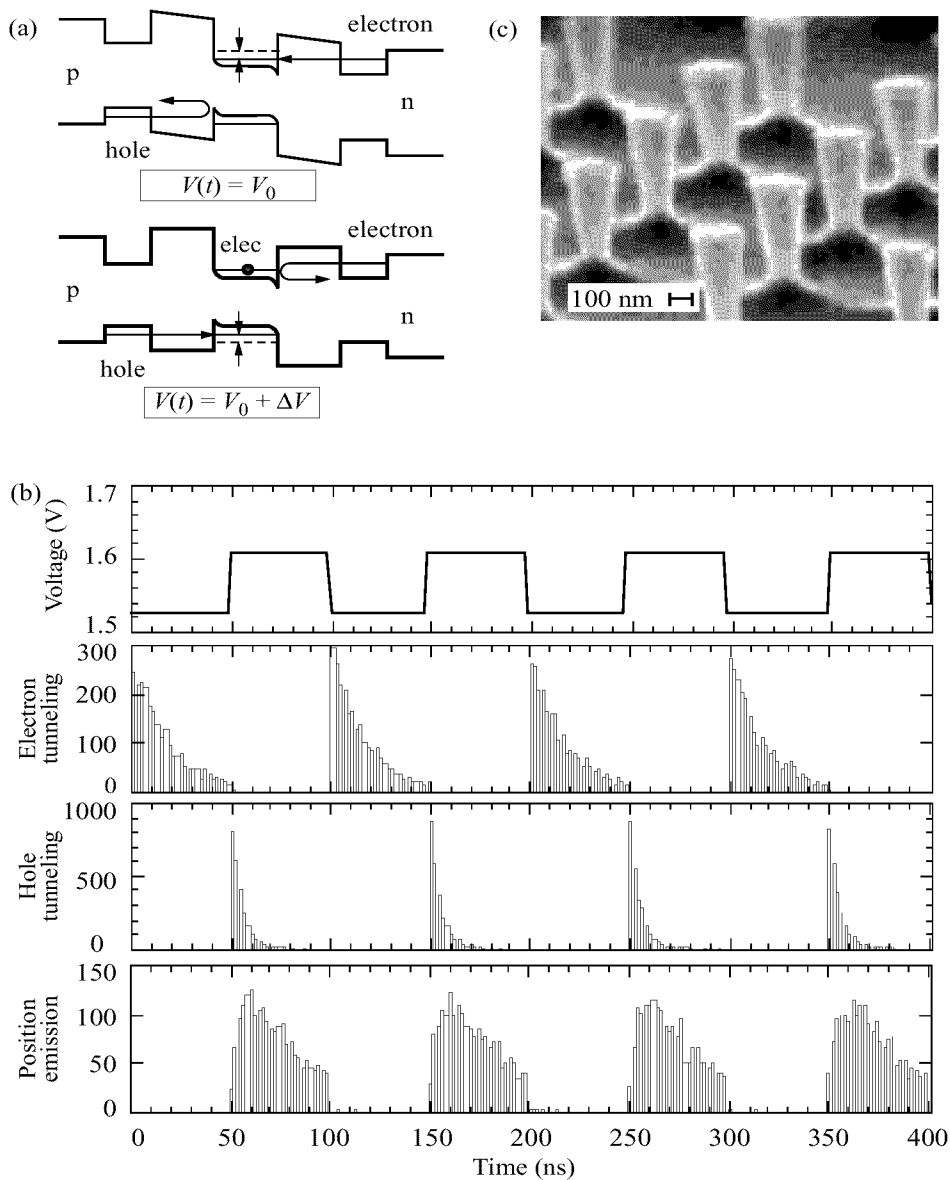


**Fig 1.** The principle of a single-photon turnstile device. (a) The energy band diagrams of the device at two bias voltages. (b) Monte-Carlo numerical simulation results for the statistical distribution of single-electron tunneling, single-hole tunneling, and single-photon emission. (c) Scanning electron microscope (SEM) photograph of typical etched post structures.

lateral size of the device is reduced to increase the single-charging energy  $e^2/2C_i$ , where  $C_i$  ( $i = n$  or  $p$ ) is the capacitance between the central QW and the side QWs. The  $n$ -th electron resonant tunnel condition into an electron sub-band in the central QW is satisfied at a certain bias voltage  $V_0$ . When the  $n$ -th electron tunnels, the Coulomb blockade effect shifts the electron sub-band energy to off-resonance, so that the  $(n+1)$ -th electron tunneling is inhibited. In our single-photon turnstile device described later, the number of electrons in the central quantum well switches between  $n-1$  and  $n$ , where  $n$  is approximately 10. At this bias voltage, the hole resonant tunnel condition is not satisfied, so there is no hole in the central QW. Then the bias is increased to  $V_0 + \Delta V$  to satisfy the hole resonant tunneling condition. If a single hole tunnels into the hole sub-band of the central QW, the subsequent hole tunneling is inhibited due to the Coulomb blockade effect for holes. By periodically modulating the bias voltage between the electron and the hole resonant tunneling conditions, we can periodically inject a single ( $n$ -th) electron and a single (first) hole into the central QW if the tunnel time is much shorter than the pulse duration. If the radiative recombination time of an electron-hole pair is also much shorter than the pulse duration, a single photon is always emitted per modulation cycle.

A Monte-Carlo numerical simulation of the device produces the statistics of subsequent photon emission events after a single photon is emitted at  $t = 0$  [Fig. 1(b)]. Experimental parameters such as the electron tunnel time  $\tau_e = 25$  ns, hole tunnel time  $\tau_h = 4$  ns, radiative recombination lifetime  $\tau_{ph} = 30$  ns, charging energy  $e^2/2C_n = e^2/2C_p = 1.3$  meV and thermal energy  $k_B\Theta = 4.3$   $\mu$ eV are assumed. It is shown that a single-photon emission event is localized to a short time interval immediately after a single-hole tunneling event.

### 3 Experimental results

A GaAs/AlGaAs three-QW structure sandwiched by  $n$ -type and  $p$ -type AlGaAs bulk layers was grown using the MBE technique. Post structures with diameters of 200 nm–1.0  $\mu$ m were made by electron-beam lithography followed by metal evaporation, lift-off, and  $\text{BCl}_3/\text{Cl}_2$  ECR plasma etching. An SEM micrograph of typical etched posts is shown in Fig. 1(c). The surface of the device was passivated with sulfur in a  $(\text{NH}_4)_2\text{S}$  solution and encapsulated by silicon nitride film. Finally, the structure was planarized with hard-baked photoresist and bonding pads were evaporated. The top semi-transparent metal served as the  $p$ -type contact from which an emitted photon is detected and the  $n$ -type contact was formed in the substrate.

The device was installed in a dilution refrigerator with a base temperature of 50 mK and was biased with a dc and ac voltage source. We applied a square wave ac voltage at a modulation frequency of 10 MHz and a modulation amplitude of 40 mV on top of the dc bias voltage and measured the current flowing through the device as a function of the bias voltage. A typical experimental result for a device with post diameter of 600 nm is shown in Fig. 2(a). The inset shows the current in a larger voltage scale. We observed a well-defined resonant tunneling current peak with very small background current even though the junction is so small, which indicates that a surface (leakage) current is well suppressed by the above-mentioned passivation process. Direct measurement of emitted photons from this device indicates that this resonant tunneling current produces photons with a very high internal quantum efficiency and, therefore, the non-radiative

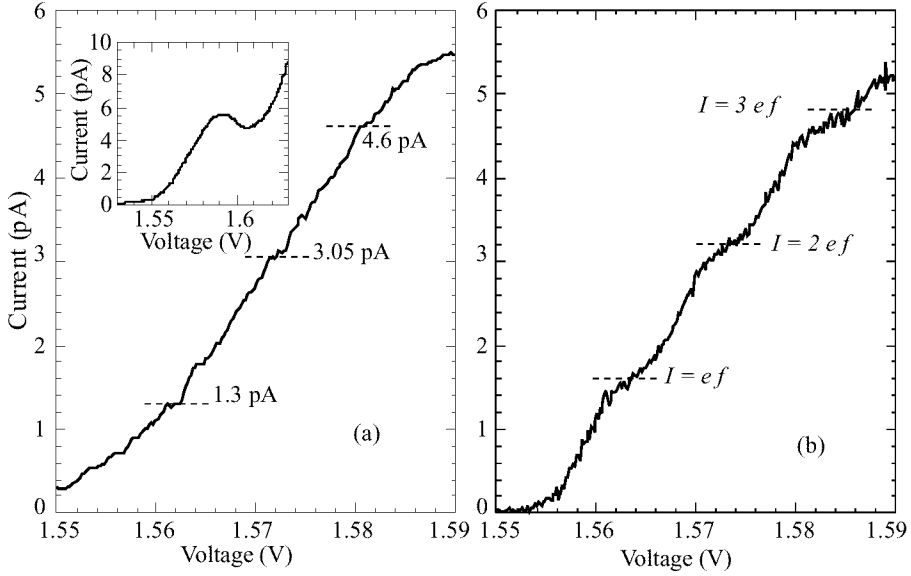


**Fig 2.** The current-voltage characteristics of the turnstile device. (a) Current vs. voltage characteristics of a 600 nm device. (b) Monte Carlo simulation result of current-voltage characteristics of the device.

recombination at the surface is negligible in our device. The tunnel current featured three plateaus near 1.4 pA, 3.1 pA, and 4.6 pA. These values correspond to  $I = \eta_n n e f$ , where  $e = 1.6 \times 10^{-19}$  C is the electron charge,  $f = 10$  MHz is the modulation frequency,  $n = 1, 2, 3$ , and  $\eta_n$  is the fidelity of the turnstile operation. The locking of the current at multiples of  $I_0 = ef$  suggests that the charge transfer through the device is strongly correlated with the external driving signal [8, 9, 10]. A slightly smaller current compared to the expected values  $I = nef$  is due to a finite missing rate of the  $n$ -th electron tunneling and the reverse tunneling rate of a hole. This is characterized by fidelity  $\eta_n$ , which is a measure of the accuracy of the turnstile operation. In our measurements,  $\eta_1 = 81\%$ ,  $\eta_2 = 95\%$ , and  $\eta_3 = 96\%$ . Figure 2(b) shows the Monte-Carlo simulation result for the actual device parameters, which reproduces the measurement result well. At the first plateau, the single ( $n$ -th) electron and the single (first) hole are injected into the central QW per driving pulse, resulting in single-photon emission. At the second plateau ( $n = 2$ ), two [ $n$ -th and ( $n + 1$ )-th] electrons and two (first and second) holes are injected into the central QW per modulation cycle, resulting in two-photon emission. At the third plateau ( $n = 3$ ), three electrons and three holes are injected per modulation cycle, resulting in three-photon emission. A non-unity fidelity  $\eta_n$  is also evident from the numerical simulation.

The emitted photon from this device is detected by a Si solid-state photomultiplier (SSPM). This detector features a high quantum efficiency of  $\sim 80\%$ , high multiplication gain of  $\sim 30,000$ , fast response time of  $\sim 2$  nsec and absolutely no multiplication noise [11]. The detector was installed on the mixing chamber of the dilution refrigerator, but the temperature was held at 5.30 K with good thermal isolation. To observe the

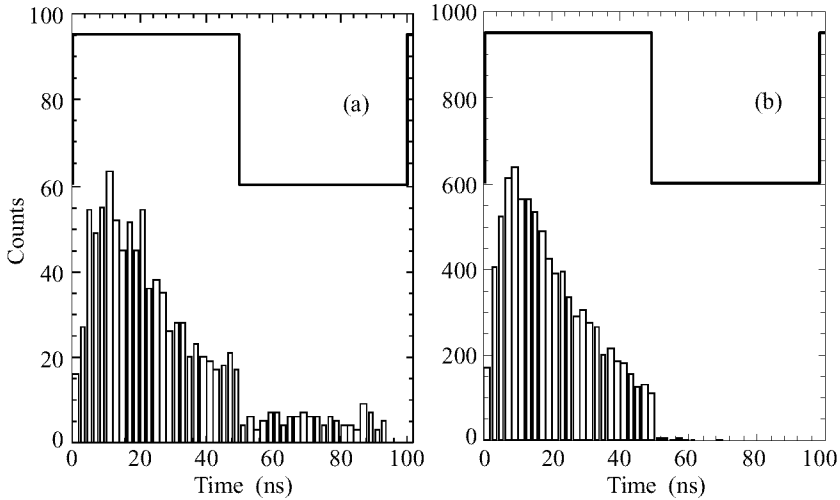


**Fig 3.** The photon emission characteristics of the turnstile device. (a) Histogram of the time interval between the rising edge of the driving ac modulation and the photon detection event on the first plateau, where a single electron and a single hole are injected per modulation cycle. (b) Monte-Carlo simulation result of the time interval for the first plateau.

correlation between the driving signal and photon emission, we measured the time interval between the rising edge of the driving pulse and the photon detection event at the first ( $I = ef$ ) plateau of the current-voltage characteristics. As mentioned before, photons are expected to be emitted soon after the junction voltage is switched to the hole resonant tunneling condition. The histograms of the measured time interval are shown in Fig. 3(a) (first plateau). The data shows that the emitted photons follow the rising edge of the driving pulse, as expected. Two time constants can be identified from this data: The rapid increase of the histogram gives the finite hole tunneling time ( $\tau_h \simeq 4$  ns), and the slow decay of the histogram gives the radiative recombination lifetime ( $\tau_{ph} \simeq 30$  ns). The sharp cut-off of photon emission following the falling edge of the driving pulse in Fig. 3(a) is due to reverse hole tunneling and reduces the fidelity of turnstile operation. The experimental result, except for a small dark count (background), is well reproduced by the Monte-Carlo simulation using the same numerical parameters, as shown in Fig. 3(b).

#### 4 Conclusion

The result reported here is the first generation of a heralded single photon, two photons, and three photons with a well-regulated time interval. Such a nonclassical photon source can provide an efficient source for future quantum information technology and a useful tool for fundamental tests of quantum mechanics.

#### References

- [1] R. Hanbury Brown and R. Q. Twiss *Nature* **177** 27 (1956).
- [2] M. Reznikov, M. Heiblum, H. Shtrikman and D. Mahalu *Phys. Rev. Lett.* **75** 3340 (1995).

- [3] A. Kumar, L. Saminadayar, D. C. Glattli, Y. Jin and B. Etienne *Phys. Rev. Lett.* **76** 2778 (1996).
- [4] R. C. Liu, B. Odom, Y. Yamamoto and S. Tarucha *Nature* **391** 263 (1998).
- [5] A. Imamoglu and Y. Yamamoto *Phys. Rev. Lett.* **72** 210 (1994).
- [6] A. Imamoglu, H. Schmidt, G. Woods and M. Deutsch *Phys. Rev. Lett.* **79** 1467 (1997).
- [7] Y. Yamamoto *Nature* **390** 17 (1997).
- [8] P. Delsing, K. K. Likharev, L. S. Kuzmin and T. Claeson *Phys. Rev. Lett.* **63** 1861 (1989).
- [9] L. J. Geerligs et al. *Phys. Rev. Lett.* **64** 2691 (1990).
- [10] L. P. Kouwenhoven et al. *Phys. Rev. Lett.* **67** 1626 (1991).
- [11] J. Kim, Y. Yamamoto and H. H. Hogue *Appl. Phys. Lett.* **70** 2852 (1997).